

Relating Response Inhibition, Brain Connectivity, and Freezing of Gait in People with Parkinson's Disease

Daniel S. Peterson^{1,2,*} , Katrijn Smulders³, Martina Mancini⁴, John G. Nutt⁴, Fay B. Horak^{4,5} and Brett W. Fling⁶

¹College of Health Solutions, Arizona State University, Phoenix, AZ, USA

²VA Phoenix Health Care System, Phoenix, AZ, USA

³Department of Research, Sint Maartenskliniek, Nijmegen, the Netherlands

⁴Department of Neurology, Oregon Health & Science University, Portland, OR, USA

⁵VA Portland Healthcare Systems, Portland, OR, USA

⁶Department of Health and Exercise Science, Colorado State University, Fort Collins, CO, USA

(RECEIVED August 18, 2020; FINAL REVISION October 9, 2020; ACCEPTED October 21, 2020; FIRST PUBLISHED ONLINE December 9, 2020)

ABSTRACT

Objective: Freezing of gait (FoG) in Parkinson's disease (PD) has been associated with response inhibition. However, the relationship between response inhibition, neural dysfunction, and PD remains unclear. We assessed response inhibition and microstructural integrity of brain regions involved in response inhibition [right hemisphere inferior frontal cortex (IFC), bilateral pre-supplementary motor areas (preSMA), and subthalamic nuclei (STN)] in PD subjects with and without FoG and elderly controls. **Method:** Twenty-one people with PD and FoG (PD-FoG), 18 without FoG (PD-noFoG), and 19 age-matched controls (HC) completed a Stop-Signal Task (SST) and MRI scan. Probabilistic fiber tractography assessed structural integrity (fractional anisotropy, FA) among IFC, preSMA, and STN regions. **Results:** Stop-signal performance did not differ between PD and HC, nor between PD-FoG and PD-noFoG. Differences in white matter integrity were observed across groups ($.001 < p < .064$), but were restricted to PD *versus* HC groups; no differences in FA were observed between PD-FoG and PD-noFoG ($p > .096$). Interestingly, worse FoG was associated with higher (better) mean FA in the r-preSMA, ($\beta = .547, p = .015$). Microstructural integrity of the r-IFC, r-preSMA, and r-STN tracts correlated with stop-signal performance in HC ($p \leq .019$), but not people with PD. **Conclusion:** These results do not support inefficient response inhibition in PD-FoG. Those with PD exhibited white matter loss in the response inhibition network, but this was not associated with FoG, nor with response inhibition deficits, suggesting FoG-specific neural changes may occur outside the response inhibition network. As shown previously, white matter loss was associated with response inhibition in elderly controls, suggesting PD may disturb this relationship.

Keywords: Inhibition, Stop-signal task, Freezing of gait, Parkinson's disease, Neuroimaging, Diffusion tensor imaging

INTRODUCTION

Freezing of gait (FoG), described as, a “brief, episodic absence or marked reduction of forward progression of the feet despite the intention to walk” (Nutt et al., 2011, p. 734), is a debilitating feature of Parkinson's disease (PD) that restricts mobility (Walton et al., 2015). Although multifactorial, one hypothesized factor in FoG is altered cognition. The “cognitive control hypothesis” suggests that altered cognitive function may contribute to or precipitate a FoG event (Nieuwboer & Giladi, 2013). Indeed, deficits have

been observed in motor inhibition and set switching in those with FoG (Bissett et al., 2015; Naismith, Shine, & Lewis, 2010; Smulders, Esselink, Bloem, & Cools, 2015; Vandenberghe et al., 2011). Although the tasks used in these studies are varied and tap into multiple cognitive processes, they share an overlapping component whereby the participant is confronted with a stimulus that triggers two competing responses. Resolution of this conflict requires inhibition of one response and facilitation of the other. An impaired ability to appropriately inhibit tasks or switch across tasks could overwhelm the nervous system and result in a neural “traffic jam” that expresses as a freezing episode (Lewis & Barker, 2009).

Inhibition (or cancellation) of a preplanned response can be assessed with stop-signal test paradigms. In these paradigms, a stimulus cues a motor response, and then in about 25% of the trials, a second stimulus is presented to halt the motor

*Correspondence and reprint requests to: Daniel Peterson, PhD, Assistant Professor, College of Health Solutions, Arizona State University, 425 N 5th St., Phoenix, AZ 85004, USA. Mailcode 9020, Tel.: +1 602 827 2279; Fax: +1 602 827 2253. Email: daniel.peterson1@asu.edu

response. Converging evidence suggests that inhibition in stop-signal paradigms is facilitated by a specific network consisting of the right hemisphere's inferior frontal gyrus (r-IFC), bilateral pre-supplementary motor areas (preSMA), and subthalamic nuclei (STN) (Aron, Robbins, & Poldrack, 2014; Coxon, Van Impe, Wenderoth, & Swinnen, 2012; Rae, Hughes, Anderson, & Rowe, 2015).

People with PD and FoG exhibit altered supra-spinal neuronal connectivity. Although results are somewhat mixed and need confirmation in larger samples, recent studies have indicated that changes in structural (Fling et al., 2013) and functional (Bharti et al., 2019; Fling et al., 2014) connectivity may be more pronounced in the right hemisphere in people with FoG compared to people without FoG, and may overlap the response inhibition network (Fling et al., 2013, 2014; Gilat et al., 2015). Given the preliminary evidence of deficits in stop-signal-related neural circuitry in people with FoG, as well as the hypothesized relationship between inhibition and FoG, it is plausible that stop-signal ability is related to FoG. However, evidence on this topic is mixed. For example, Bissett and colleagues showed that performance on a stop-signal paradigm was impaired in people with PD who experience FoG compared to people with PD without FoG (Bissett et al., 2015), while Stefanova et al. found no differences across groups (Stefanova et al., 2014). Together, these conflicting results reflect an incomplete understanding of the links (or lack thereof) between inhibitory control and freezing behavior, as well as the neural circuitry that underlie them.

Therefore, the primary objective of the current study was to characterize the relationship between FoG, inhibition (measured via a stop-signal paradigm), and structural connectivity in the response inhibition network in people with PD with and without FoG. Specifically, in people with PD with and with FoG, we: (1) compared response inhibition performance with a Stop-Signal Task (SST), (2) compared microstructural integrity within the response inhibition network (r-IFC, preSMA, and STN), and (3) correlated stop-signal performance with microstructural integrity in this response inhibition network. We hypothesized that people with FoG would show poorer response inhibition performance, measured by longer Stop-Signal Reaction Times (SSRT), and poorer microstructural integrity within the right hemisphere's response inhibition network. We also hypothesized that response inhibition performance would be correlated with white matter integrity of the response inhibition network.

METHODS

Participants

Sixty people were recruited (41 people with PD and 19 healthy adults). Convenience sampling was used for participant recruitment. Specifically, participants were contacted by existing participant databases. We also relied on fliers placed in the community and clinician referral. Finally, some participants were recruited via the Parkinson's Center of Oregon at

the Oregon Health & Science University. Of the 41 PD participants, 20 patients self-reported FoG via the New Freezing of Gait Questionnaire (NFoG-Q1 = 1) (Nieuwboer et al., 2009), and thus were included in the PD-FoG group, and 21 age- and gender-matched PD patients without report of FoG were included in the PD-noFoG group. One subject without self-reported FoG showed FoG during turning (confirmed by a movement disorders neurologist; J.N.) and was added to the PD-FoG group.

Inclusion criteria were idiopathic PD according to the UK Brain Bank criteria (Hughes, Daniel, Kilford, & Lees, 1992) confirmed by movement disorders neurologists, Hoehn and Yahr (H&Y) (Hoehn & Yahr, 1967) stages II–IV, aged 50–90 years, and ability to walk or stand for 2 min without an assistive device. Exclusion criteria were implanted electrodes for deep brain stimulation, dementia (Montreal Cognitive Assessment < 18) (Nasreddine et al., 2005), or contraindications for MRI scans. Finally, participants were excluded if they presented with any peripheral, central nervous system, or musculoskeletal disorders affecting gait or balance other than PD. Severity of parkinsonian signs was assessed by trained raters using the Movement Disorders Society – Unified Parkinson's Disease Rating Scale Part III (MDS-UPDRS-III) (Goetz et al., 2008). Two subjects with PD (both PD-noFoG) had invalid SST results. Specifically, these participants' probability to stop was above 0.7, the cutoff for validity and interpretability of outcomes such as the SSRT (Verbruggen et al., 2019). After the removal of these two participants, the final numbers were 21 PD-FoG, 18 PD-noFoG, and 19 healthy subjects (Table 1).

Data were collected in compliance with the regulations of OHSU and the Helsinki Declaration, and the study was approved by the OHSU Institutional Review Board. Each subject gave informed written consent before participating.

Protocol and Outcomes

All assessments [clinical assessments (MDS-UPDRS-III, MoCA, etc.)], objective assessment of FoG, SSRT, and neuroimaging were conducted in the OFF medication state, after a minimum of 12 hr withdrawal of all PD medications (dopamine replacement and agonists). Assessments occurred in the morning to reduce the OFF medication burden for the PD participants.

Objective Assessment of Freezing of Gait

We used objective and continuous measures to assess severity of FoG as described previously (Mancini et al., 2017). Briefly, a FoG ratio was calculated from acceleration of the shins (measured via inertial sensors, Opals by APDM) during a 1-minute turning task in which subjects made alternating 360° turns as fast as safely possible (Figure 1). Power spectral density from anteroposterior acceleration signals was calculated. Then, a FoG ratio was calculated as the ratio of total power in the "freezing band" (3–8 Hz) and the "locomotion band" (0.5–3 Hz). Higher freezing ratios indicate higher

Table 1. Demographic and clinical characteristics of all participants

	PD-FoG	PD-noFoG	HC	<i>p</i>
<i>n</i>	21	18	19	
Age	68 ± 8	67 ± 7	69 ± 8	.978
Gender (%M)	84 %	83 %	86 %	.965 ²
MoCA	26 ± 4	26 ± 4	27 ± 2	.571
MDS UPDRS-III (0–132)*	43 ± 15	34 ± 11	NA	.045 ¹
Disease duration	10 ± 7	5 ± 4	NA	.011 ¹
NewFOGQ (0–24)	14.1 (7.0)			
FoG ratio	4.08 (7.60)	0.98 (0.61)	0.39 (0.24)	<0.001
H&Y				
2	15 (71 %)	17 (94 %)		.156 ^{1,2}
3	4 (19 %)	1 (6 %)		
4	2 (10 %)	0 (16 %)		

MoCA=Montreal Cognitive Assessment; MDS UPDRS-III=Movement Disorders Society – Unified Parkinson’s Disease Rating Scale Part III (motor examination); H&Y=Hoehn & Yahr. For MDS-UPDRS-III, NFOGQ, FoG ratio, and H&Y, larger values reflect worse symptoms or performance; for MoCA, larger values reflect better cognitive performance.

¹Comparing PD-noFoG and PD-FoG; ²Chi-square test; *MDS UPDRS-III captured while in the “OFF” medication state.

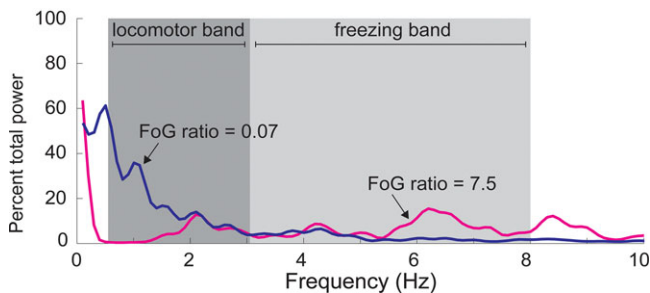


Fig. 1. Calculation of FoG ratio. The FoG ratio is calculated from anterior–posterior accelerations of the shins while turning. The power spectral density of this signal is plotted here. Gait stepping during turning occurs at 0.5–3 Hz (locomotor band), whereas high-frequency movements reflect “trembling of the knees” during freezing episodes (3–8 Hz, freezing band). The FoG ratio is calculated as the ratio between the area under the power density curve in the freezing band divided by the area under the curve of the locomotor band. Two example trials are presented in which no FoG (blue, FoG ratio of 0.07) and multiple FoG episodes occurred (magenta, FoG ratio of 7.5).

severity of FoG. FoG ratio has been shown to correlate well with FoG severity as measured by a video review of turning in place (Mancini et al., 2017).

Stop-Signal Reaction Time Task

Response inhibition was assessed using the stop-signal paradigm (Verbruggen, Logan, & Stevens, 2008). The test consists of 1 practice block (32 trials) and 3 experimental

blocks (each 64 trials). Short rest breaks occurred between blocks. Subjects were seated comfortably in front of a 38 × 30 cm monitor, and were instructed to use their left and right hands, respectively, to press the “Z” key (bottom left corner of the keyboard) for a square and the “/” key (bottom right side of the keyboard) for a circle as fast as possible without errors. Wrists were resting comfortably on a table for all trials. The stimulus was presented until the subject had responded, with a maximum reaction time of 1250 ms. Interstimulus intervals were 2000 ms. In 25% of the trials, a stop signal was presented as an auditory tone. Subjects had to stop their response in these trials. The interval between the stimulus and the stop signal depended on the success of the previous stop trial using a staircase tracking procedure. Successful stop trials led to a 50 ms increase in stimulus-stop delay (SSD), whereas unsuccessful stop trials led to 50 ms shorter SSD, resulting in an overall probability of successful stopping around 50%. Initial SSD was set at 250 ms. Participants were reminded not to wait for a stop signal to occur between each block, and were provided feedback after each block regarding the percentage of stop trials actually stopped. These measures are in-line with recent guidelines regarding SST administration (Verbruggen et al., 2019).

The SSRT was calculated using the integration method (Verbruggen, Chambers, & Logan, 2013). First, all reaction times of nonstop trials were rank-ordered. The probability of successfully inhibiting a response whenever a stop signal was present, $p(\text{stopsignal})$, was calculated for every subject. The $p(\text{stopsignal})$ was then used to select the corresponding RT (i.e., if $p(\text{stopsignal}) = 45\%$, stop RT is RT at 45th percentile). SSRT was calculated as stop RT – mean SSD. Two PD-FoG subjects were excluded because of $p(\text{stopsignal}) > 0.7$, indicating invalid tests (Verbruggen et al., 2019). Accuracy (correct left–right responses) was also calculated.

Image Acquisition

Neuroimaging scans occurred in a 3.0T Siemens Magnetom Tim Trio scanner with a 12-channel head coil at Oregon Health & Science University’s Advanced Imaging Research Center. We acquired one high-resolution T1-weighted MP-RAGE sequence (orientation = Sagittal, echo time = 3.58 ms, repetition time = 2300ms, 256 × 256 matrix, resolution 1.0 × 1.0 × 1.1 mm.; scan time = 9 min 14 s). High-angular-resolution diffusion images (HARDI) were also collected using a 72-gradient direction, whole-brain echo-planar imaging sequence (TR = 7100 ms, TE = 112 ms, field of view = 230 × 230 mm², *b* value = 3000 s/mm², isotropic voxel dimensions = 2.5 mm³) and 10 images in which the *b* value was equal to zero. A static magnetic field map was also acquired using the same parameters as the diffusion-weighted sequence.

Diffusion Tensor Imaging Analysis

Diffusion data were processed using the tools implemented in FSL (Version 5.0; www.fmrib.ox.ac.uk/fsl).

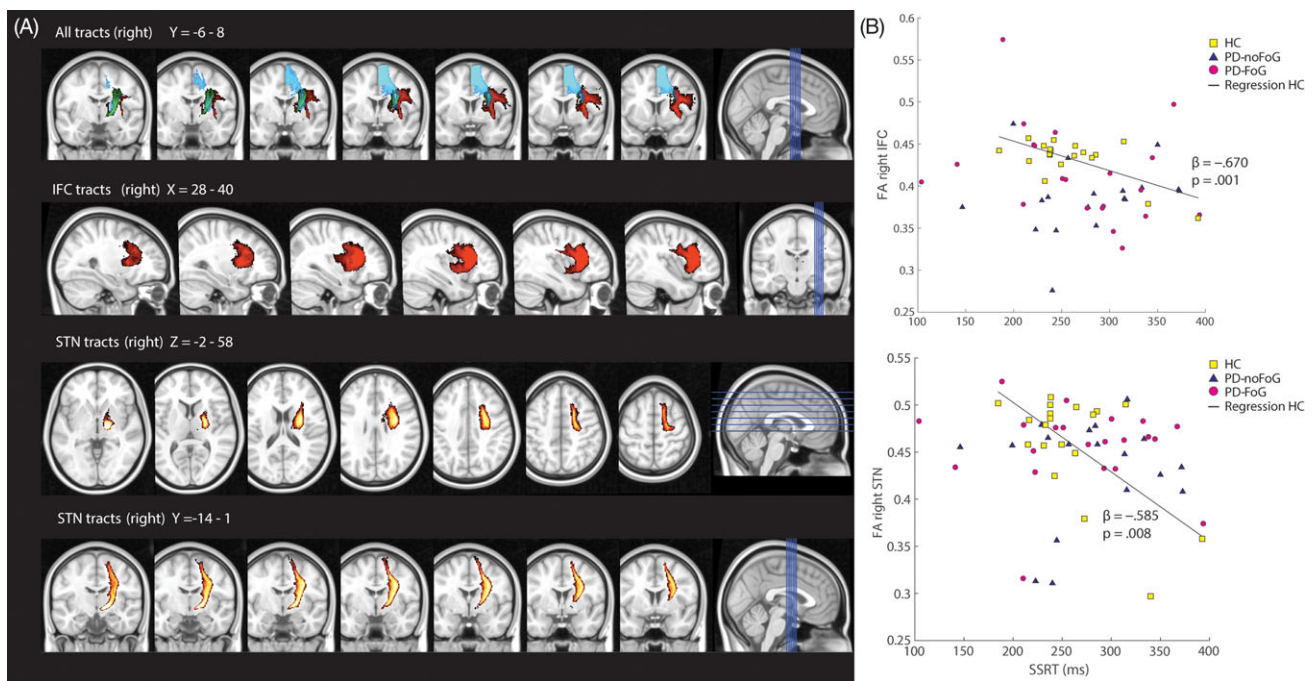


Fig. 2. (A). Identified white matter tracts within the response inhibition network. In the upper panel, all tracts are shown between the right hemisphere's inferior frontal cortex (IFC, in red), pre-supplementary motor area (preSMA, in blue), and subthalamic nucleus (STN, in green). All tracts are thresholded to include fibers where at least 95% of the participants had identifiable tracts. In the lower panels, the IFC and STN tracts are shown separately. (B). Correlations between behavioral response inhibition performance and microstructural integrity in the response inhibition network. Higher mean fractional anisotropy (FA) of the identified right IFC (top) and STN (bottom) tracts correlated with higher Stop-Signal Reaction Times (SSRT) in neurotypical, healthy controls (HC; see regression line), but not in subjects with Parkinson's disease (PD) with or without FoG. Presented β values for the relationship between FA and SSRT in panel B represent correlations between these variables while controlling for age and gender.

Briefly, diffusion data were corrected for eddy current distortions and motion artifacts, averaged to improve signal-to-noise ratio, and skull-stripped (Eickhoff et al., 2010). For each individual, the fractional anisotropy (FA) images were normalized into Montreal Neurological Institute (MNI) space by using a linear (affine) registration and Fourier interpolation through the FMRIB linear image registration tool. A probabilistic diffusion model that accommodates crossing fibers was applied to calculate fiber tract probability distributions at each voxel to identify tract quality (Behrens, Berg, Jbabdi, Rushworth, & Woolrich, 2007; Behrens et al., 2003). Probabilistic tractography was run from cortical seed masks, constrained by a target and termination mask, to delineate the following tracts: (1) r-IFC to r-preSMA; (2) r-IFC to r-STN; (3) r-preSMA to r-STN; (4) l-preSMA to l-STN; (5) l-IFC to l-preSMA; and (6) l-IFC to l-STN. Seed masks for probabilistic tractography were determined in MNI space using procedures previously outlined (Coxon et al., 2012) and transformed to subject diffusion space using the inverse of the FA registrations.

FA Region of Interest Analysis

Due to the strong body of literature identifying r-IFC, preSMA, and STN as critical nodes in a neural network for response inhibition (Aron et al., 2014; Coxon et al., 2012;

Rae et al., 2015), we utilized an *a priori* ROI-based approach. Resultant fiber tracts were thresholded, transformed into MNI space, binarized, and summed across participants (Aron, Behrens, Smith, Frank, & Poldrack, 2007). Voxels that were present in >95% of the participants' maps were retained (Figure 2A). For ease of interpretation, the ROIs are labeled according to the common seed/target node (e.g., the r-IFC ROI was determined by the multiplication of the tract between r-IFC and r-preSMA and the tract between r-IFC and r-STN). Thus, the value for each ROI can be thought to reflect the integrity of white matter projections to/from the other neural nodes (e.g., r-IFG contains voxels projecting to/from both r-preSMA and r-STN). The resulting MNI space tract ROIs were subsequently used to extract the mean from each subjects' FA image. FA is a rotationally invariant index that ranges from 0 (*isotropic*) to 1 (*anisotropic*), higher FA values indicating higher white matter integrity.

Statistical Analysis

Demographic, clinical, and response inhibition differences among groups were tested with ANOVAs (comparing all groups), independent *t*-tests (PD-FoG vs. PD-noFoG), or chi-square for categorical variables.

FA data and some behavioral (i.e., SSRT) data were non-normally distributed. Therefore, nonparametric tests were

used to assess across-group differences in FA and behavioral data. Specifically, Kruskal–Wallis tests assess overall group effects, and Mann–Whitney U tests assessed pre-planned, across-group comparisons (HC vs. PD-noFoG, HC vs. PD-FoG, and PD-noFoG vs. PD-FoG). Hodges–Lehmann CI estimates were calculated for these assessments.

Regression models were run in PD-FoG to analyze the association between ROI FA values and FoG ratio, adding age, gender, and disease duration as covariates. FoG ratio was positively skewed across all PD subjects with a median of 1.22 (range from 0.23 to 34.48). Hence, logarithmic transformation (ln) of the FoG ratio was used to equalize variances for this analysis.

The relationship between FA of each ROI and the SST behavior was analyzed using regression models with dependent variable SSRT and ROI FA was the independent variable. Age and gender were included as covariates. Planned within-group (HC, PD-noFoG, and PD-FoG) models were also run. Despite non-normal distributions of some FA outcomes, residuals of the regression models were *not skewed* (Shapiro–Wilk test outcomes $p > .205$ for all models). Nonetheless, to identify potential outlier bias, in all instances where significance between the FA ROI and SSRT was observed, Cook’s distance values were calculated. Model outcomes with high-leverage data points excluded are presented.

RESULTS

Results describing SSRT performance across groups, structural integrity across groups, and the relationship between SSRT and structural integrity are presented in turn.

SSRT Performance

Means and statistical outcomes of SST performance are shown in Table 2. Across all subjects, the average RT of Go trials (692 ± 172 ms) and was longer than the average RT of the failed stop trials (627 ± 155 ms; $t_{1,57} = 10.97$, $p < .001$). Accuracy rates were high and not significantly different among groups ($F_{2,55} = 1.49$, $p = .235$). Average SSRT of the whole sample was 268 ± 61.6 ms. Mean SSRT also did not differ between groups (main group effect: $F_{2,55} = 0.38$, $p = .686$).

Microstructural Integrity of the Stopping Network

Across and within-group analyses of all FA values can be found in Table 3. Models showed statistically significant differences across groups for r-IFC ($p = .005$), l-IFC ($p = .003$), l-preSMA ($p = .001$), and l-STN ($p = .004$), and trends toward significance in r-preSMA ($p = .057$) and r-STN ($p = .064$). Within-group analyses showed that: (1) HC exhibited larger (better) FA compared to PD-noFoG across all ROIs ($0.001 < p < .042$), (2) HC – PD-FoG differences were less robust, and more commonly observed

Table 2. Stop-Signal Task (SST) output means and statistical comparisons across the three groups: PD who freeze (PD-FoG), PD who do not freeze (PD-noFoG), and healthy controls (HC). SST outcomes (and in particular, SSRT) were largely similar across all groups. Nonparametric Kruskal–Wallis, Mann–Whitney U, and Hodges–Lehmann assessments were used due to the non-normal distribution of data

SST outcome	PD-FoG (n = 21)	PD-noFoG (n = 18)	HC (n = 19)	All groups ^a			Within-group, <i>post hoc</i> assessments											
				M ± SD	χ ²	p	HC versus PD-noFoG ^b			HC versus PD-FoG ^b			PD-FoG versus PD-noFoG ^b					
							U	p	CI ^c	U	p	CI ^c	U	p	CI ^c			
SSRT	267 ± 73	278 ± 61	260 ± 48	1.31	.518	.134	.261	19.21	[−58.21, 14.64]	175	.507	−12.40	[−55.95, 27.19]	170	.592	10.06	[−35.65, 56.74]	
Accuracy	94 ± 8	94 ± 6	97 ± 5	4.42	.110	105	.042	2.14	[.00, 5.57]	144.5	.131	1.42	[.00, 4.90]	170	.592	−.70	[−3.55, 2.11]	
Go RT	728 ± 155	698 ± 180	647 ± 182	4.68	.096	169	.951	−64.19	[−167.0, 45.76]	120	.031	−78.11	[−222.79, 10.83]	136	.135	−37.78	[−152.01, 77.23]	
SSD	428 ± 172	393 ± 192	372 ± 204	1.50	.473	157	.671	−33.02	[−151.6, 84.09]	156	.233	−68.96	[−191.67, 41.67]	162	.447	−43.96	[−162.96, 87.22]	
Failed stop RT	657 ± 141	634 ± 174	588 ± 150	3.07	.216	134	.261	−46.00	[−134.8, 41.44]	135	.081	−70.00	[−171.00, 10.29]	173	.652	−29.04	[−133.72, 70.51]	
p (stop/signal)	.56 ± .05	.53 ± .07	.52 ± .04	3.28	.194	134	.261	0.00	[−.03, .05]	136	.085	.031	[0.00, 0.062]	161	.430	.03	[−.011, .064]	

SSRT=Stop Signal Reaction Time; Go RT=Reaction time for “go” trials; SSD=Stop Signal Delay; p(stop/signal)=probability of stopping a trial with a stop signal. ^aKruskal–Wallis Test; ^bMann–Whitney U Test; ^cHodges–Lehmann CI estimate.

Table 3. Across-group comparisons of microstructural integrity in *a priori* regions of interest

ROI	PD-FoG (n = 21)		PD-noFoG (n = 18)		HC (n = 19)		All groups ^a			Within-group, <i>post hoc</i> assessments						
	M ± SD		M ± SD		M ± SD		χ ²	p	HC versus PD-noFoG ^b			PD-FoG versus PD-noFoG ^b				
									χ ²	p	CI ^c	χ ²	p	CI ^c		
r-IFC	.41 ± .06	.39 ± .04*	.43 ± .02	.39 ± .04	.43 ± .02	10.7	.005	11.4	.001	.052 [.038,.063]	3.2	0.72	.028 [−.003,.054]	1.8	.185	−.022 [−.055,.009]
r-preSMA	.40 ± .04	.39 ± .04	.42 ± .05	.39 ± .04	.42 ± .05	5.7	.057	4.1	.042	.034 [.001,.058]	4.4	.036	.029 [.004,.055]	.003	.955	−.001 [−.029,.022]
r-STN	.46 ± .04	.43 ± .06	.46 ± .06	.43 ± .06	.46 ± .06	5.5	.064	4.5	.033	.028 [.000,.048]	1.1	.297	.014 [−.015,.029]	2.8	.096	−.017 [−.042,.002]
l-IFC	.39 ± .04*	.38 ± .02*	.44 ± .06	.38 ± .02*	.44 ± .06	11.5	.003	10.0	.002	.071 [.056,.094]	6.4	.011	.065 [.042,.084]	.92	.338	−.006 [−.019,.007]
l-preSMA	.39 ± .02*	.38 ± .02*	.45 ± .05	.38 ± .02*	.45 ± .05	14.9	.001	11.0	.001	.083 [.055,.102]	10.5	.001	.077 [.050,.096]	1.03	.310	−.004 [−.014,.005]
l-STN	.42 ± .04	.40 ± .02*	.45 ± .06	.40 ± .02*	.45 ± .06	11.1	.004	9.6	.002	.065 [.040,.091]	4.5	.033	.047 [.007,.068]	2.76	.096	−.014 [−.019,0.007]

^aKruskal–Wallis Test; ^bMann–Whitney U Test; ^cHodges–Lehmann CI estimate.

Table 4. Regression models to associate FoG severity (ln FoG ratio) with FA values of the ROIs in PD with FoG

n = 21	B (SE)	95% CI	β	p
r-IFC	0.14 (4.92)	[−.027,.027]	.006	.978
r-preSMA	17.47 (5.43)	[.004,.032]	.547	.015
r-STN	14.04 (4.95)	[.006,.042]	.514	.012
l-IFC	2.92 (8.00)	[−.014,.019]	.089	.720
l-preSMA	12.63 (14.41)	[−.003,.010]	.175	.396
l-STN	3.35 (7.27)	[−.014,.022]	.110	.652

in the left hemisphere ROIs (0.001 < p < .033) than the right hemisphere ROIs (0.036 < p < .72), and (3) no significant differences were observed between PD-FoG and PD-noFoG in FA in any ROIs (0.096 < p < .955).

Microstructural Integrity of the Response Inhibition Network and Behavioral Response Inhibition

Regression analysis outputs for models relating SSRT to FA of each ROI in all groups can be found in the Supplemental Table. Analyzing all subjects together, relationships between SSRT and STN, SMA, and IFG were modest in the right (0.081 < p < .167) and left (0.035 < p < .252) hemispheres. No significant associations between the left or right nodes and SSRT were observed in either PD group.

However, planned, within-group assessments showed that in HC, higher (i.e., better) FA values of the right hemisphere were related to faster SSRTs (r-IFC: B = −1301 (SE 332), p = .001; r-STN: B = −495 (SE 162), p = .008; Figure 2B). None of the left hemispheres nodes associated significantly with SSRT in healthy subjects. For the HC models, one participant was noted to contribute a data point that exhibited a notably large Cook’s distance value (>4/(n − k − 1) (Hair, Anderson, Tatham, & Black, 1998)) for r-IFC, r-SMA, and r-STN (0.44, 0.34, and 0.37, respectively). Removal of this data point reduced the significance of each of the FA–SSRT relationships (r-STN: p = .044, r-SMA: p = .079; r-IFC: p = .064). For the l-SMA total group model, one participant had a large Cook’s value (0.12). Removal of this participant slightly increased the significance of the model (p = .023 after removal; see Supplemental Table for details).

Severity of FoG and Integrity of the Response Inhibition Network

The FoG ratio correlated with NFoG-Q total score (r = .641, p = .002) and was significantly larger in PD-FoG than PD-noFoG (p = .028) or neurotypical adults (<.001). FA values of the r-preSMA and r-STN were significantly associated with the FoG ratio (p = .015 and .012, respectively; Table 4), indicating that larger tract integrity is associated with higher (i.e., worse) FoG ratio (B = 17.47 (5.43),

$p = .015$). Neither the r-IFC nor any of the left hemisphere nodes were associated with the FoG ratio.

DISCUSSION

Our results did not support the hypothesis that FoG is associated with response inhibition deficits or that microstructural integrity of the right hemisphere's IFC-preSMA-STN circuitry is disproportionately altered in PD-FoG. First, in contrast to our expectation, PD subjects with FoG did not have poorer SST performance or poorer structural integrity within the predefined response inhibition network compared to those without FoG. Second, the integrity of white matter tracts within the right IFC-preSMA-STN network was *higher* in subjects with more severe FoG. Third, we observed the expected positive relationship between stopping network structural integrity and stopping behavior, but only in neurotypical older adults.

Behavioral Differences between PD with and without FoG

Our results suggest that neither PD (generally) or the presence of FoG within the PD group resulted in poorer efficiency in response inhibition, measured as SST performance. Previous work has yielded inconsistent results regarding the effect of PD or FoG on stopping performance. For example, some studies have reported longer (worse) SSRT in PD compared to healthy subjects (Di Caprio, Modugno, Mancini, Olivola, & Mirabella, 2020; Gauggel, Rieger, & Feghoff, 2004; Manza et al., 2018; Obeso et al., 2011, 2014; Wylie et al., 2018), and others reported no differences, consistent with our findings (Bissett et al., 2015; Claassen et al., 2015; Kohl et al., 2015; Vriend et al., 2015). Two previous reports investigated the impact of freezing status on SSRT performance. First, and consistent with the current report, Stefanova et al. measured SSRT performance in people with ($n = 30$) and without FoG ($n = 36$), showing *no differences* across groups (Stefanova et al., 2014). However, Bisset et al. measured SSRT in neurotypical adults ($n = 21$), people with ($n = 20$), and without FoG ($n = 22$). They noted that while people with PD, on the whole, did not have worse SSRT times compared to neurotypical adults, a pre-planned comparison between people with and without FoG exhibited a subtle, but significant, worsening in SSRT in those with FoG.

The reason for the discrepancy in results when comparing FoG and non-FoG groups is unclear, but could be related to at least three differences between our and Bisset et al.'s paradigms. First, the mode of stop-signal presentation was different across studies, as Bisset and colleagues provided a visual (color change) stop signal, while the protocol in our study and that of Stefanova et al. was auditory. Although speculative, differences in the salience of the stimulus, or specific processing impairments of visual, but not auditory, stimuli in subjects with PD with FoG may have contributed to the discrepancy in

results (Davidsdottir, Cronin-Golomb, & Lee, 2005; Fearon, Butler, Newman, Lynch, & Reilly, 2015). Second, unlike Bisset et al., participants in our study completed the SST while in the "Off" levodopa state. Although the effect of dopamine on SSRT times has been mixed (Claassen et al., 2015; Manza et al., 2018; Obeso et al., 2011; Wylie et al., 2018), it is possible that dopamine replacement therapy impairs SSRT performance. Finally, Bisset and colleagues also measured (and included in their analysis) SSRT times with the feet as an effector (in addition to the hands). While there was no effector by group interactions observed, the inclusion of these data may have contributed to the significance observed in that study. In sum, while additional work will be necessary to provide consensus, the existing literature suggests FoG status likely has a relatively modest effect on SSRT performance. Further, these studies underscore the diversity in SST methodological paradigms. For subsequent studies, the adoption of reliable and standardized methodologies (e.g., Verbruggen et al., 2019) should be applied to increase the generalizability of findings.

We selected the stop-signal paradigm as a measure of inhibition because of (1) the strong evidence of the neural circuitry involved, (2) early work indicating potential deficits in these regions in PD-FoG, and (3) potential behavioral deficits in this group. However, we recognize that using upper limb responses rather than stepping responses limits validity for the task for FoG. Interestingly, two recent studies investigated response inhibition tasks during stepping, also showing mixed results. Beaulne-Seguin et al. did not find clear inhibition deficits in freezers compared to non-freezers when instructed to execute or stop a prepared stepping response to a visual cue (Beaulne-Seguin & Nantel, 2016). Alternatively, Georgiades and colleagues asked PD participants with and without FoG to perform a virtual reality stepping task with an embedded inhibition component (Georgiades et al., 2016). Participants laid supine and tapped their feet while they were shown a first-person view moving through corridors. While tapping their feet, participants were given a visual signal to stop stepping. The authors found that people with PD and FoG took more steps after the stop signal than people without FoG, thus exhibiting more difficulty "stopping" the stepping task. There are important differences between stopping an ongoing task (stepping) *versus* a released reaction time task (as in the SSRT), which may have also contributed to the partially conflicting findings between Georgiades et al. and the current report. However, together, these efforts represent an important step in developing effector-specific and FoG-specific paradigms to further understanding of inhibitory processes relevant to FoG.

We also acknowledge "inhibition" is in itself a broad domain, which is not entirely described by the SST. Further, FoG events may be related to one's (in)ability to both inhibit a response and "switch" to another task. Switching ability, often measured by tasks such as Trails B-A, has been shown to be related to freezing in some (Factor et al., 2014; Naismith et al., 2010; Shine et al., 2013), albeit not all (Morris et al., 2020), previous work. Therefore, it is possible that the null

findings in the current study were due to a somewhat myopic view of “inhibition”, measured specifically by SST, which incompletely assesses other relevant FoG-related domains such as switching. Some research has identified neural regions associated with switching, showing partial overlap to the “stopping” network – e.g., (Sylvester et al., 2003). However, there is currently limited information relating to switching ability (e.g., Trails performance), neural regions specifically associated with switching, and FoG severity across PD-FoG and PD-noFoG groups. This information could provide additional insights into factors that contribute to FoG.

White Matter Integrity in PD with and without FoG

We restricted our current analysis to the supposed response inhibition network ROIs, only considering the overlapping tracts among the ROIs, thus providing a measure of the connection strength between each node within this network (Coxon et al., 2012). Within this *a priori* selected network, we observed subjects with PD to have poorer microstructural integrity in the IFC-preSMA-STN circuitry than healthy subjects, with particular deficits in the left hemisphere. This result is consistent with previous work showing widespread cortical and subcortical white matter dysfunction in PD (Bohnen & Albin, 2011; Isaacs et al., 2019; Uribe et al., 2018).

In contrast to our expectations, we observed no statistical differences when comparing white matter tract integrity (FA) between the IFC, preSMA, and STN in those with PD who do and do not experience FoG. Previous literature suggests that when using whole-brain analyses, people with FoG often exhibit reduced quality and structural integrity of white matter tracts compared to people without FoG, with particular changes to long associative white matter bundles and in white matter emanating from brainstem regions (e.g., pedunculopontine nucleus) (Fling et al., 2013; Vercruyssen et al., 2015). However, to our knowledge, no previous investigations focused specifically on the response inhibition network, and few, if any, whole-brain analyses identified deficits in connectivity in these specific nodes. Therefore, making comparisons to previous research is difficult. In addition, the lack of significant differences in the two PD groups specifically in the response inhibition nodes may be expected given the lack of difference in response inhibition between our cohorts.

White Matter Integrity, SSRT Performance, and FoG Severity

As noted above, although people with PD (with or without FoG) exhibited altered microstructural integrity compared to HC, no differences were observed between people with PD who do and do not freeze. Given the demonstrated link between the stopping network and SSRT performance, it is therefore not entirely surprising that freezing status did not

impact SSRT performance. However, previous results (Coxon et al., 2012) would suggest that within each group, SSRT behavior would be correlated to stopping network integrity. Indeed, consistent with previous results (Coxon et al., 2012), we did observe a correlation between SSRT outcomes structural integrity in healthy older adults in the r-IFC, r-preSMA, and l-preSMA.

However, this relationship did not persist in either PD cohort. This lack of correlation was not due to reduced variability in SSRT or structural integrity outcomes. Several possible, albeit speculative, reasons are presented. First, low correlations between the right hemisphere’s IFC-preSMA-STN circuitry and behavioral response inhibition in people with PD might be explained by the fact that most of the SSRTs variance in the SST can be explained by the actual stopping phase of the inhibition process, occurring just milliseconds before the SSRT (Boucher, Palmeri, Logan, & Schall, 2007; Wessel & Aron, 2015). Hence, processing in the r-IFC-preSMA-STN might be more related to preparatory processes such as detecting and processing the stop signal and triggering the stop response, which are essential steps for response inhibition, but has a less direct correlation with SSRT variance. Second, given the pathological state of PD patients, it is possible that other variables, not measured in the current study, such as noradrenaline or dopamine levels (Eagle, Bari, & Robbins, 2008), maybe more powerful drivers of the variability in SSRT variance than structural integrity. Finally, parkinsonian pathology causes widespread neural changes and likely results in other pathways contributing to and compensating for behavioral functions, such as response inhibition (Snijders et al., 2016). Therefore, it is possible that people with PD rely less or differently on the stopping network than healthy adults for inhibition tasks. Indeed, we observed that, in people with PD and FoG, freezing severity was *positively* correlated to stopping-network structural integrity. Although this relationship was reduced after correcting for disease severity, these findings suggest that the relationship between stopping network integrity and behavior may be altered in this population. Larger (better) than normal FA has previously been shown to reflect pathological changes related to abnormal behavior in neurological populations (Hoehn et al., 2007), further supporting this speculation. Additional work in larger samples will be necessary to determine whether the stopping network plays a similar role in inhibition tasks (such as SSRT task) in people with PD as it does in neurotypical adults.

Limitations

Our results should be interpreted in the context of the following limitations. First, we focused on mean FA values of a predefined network, and we recognize that our chosen structural integrity measure (FA) does not necessarily reflect poorer physiological connectivity between brain areas. Second, although our sample size was larger than some previous

neuroimaging studies in PD with FoG (Fling et al., 2013; Vercruyse et al., 2015), the heterogeneity commonly found in subjects with FoG calls for even larger sample sizes. Third, the stop-signal paradigm that we administered carried a small working memory component (“square is left, circle is right”) that might have been disadvantageous for PD subjects. Although accuracy was high in all groups, a paradigm with direct cues (arrows) may be preferable over indirect stimuli that we used. Fourth, as noted in the results section, one outlier contributed to the observed FA–SSRT relationship in HC. Although residuals of these analyses were normally distributed, these findings should be considered with caution. Fifth, given that PD-FoG often exhibits more severe motor symptoms, it is plausible that the SSRT comparison across PD-noFoG/PD-FoG participants may have been impacted by motor severity. However, we included disease severity (measured as MDS-UPDRS III) into the SSRT analysis. Second, the “go” reaction time outcomes were not different across the FoG and non-FoG groups, further indicating that motor symptoms were unlikely to have impacted the interpretation of SSRT data in the current study. Finally, tract quantity (i.e., the volume of white matter tracts) were unable to be evaluated in this study as it was previously (Fling et al., 2013). Rather, we focused on tract quality reflecting fiber density, axonal diameter, and myelination in white matter (i.e., FA).

CONCLUSION

In summary, our results are consistent with the literature that microstructural brain changes exist in the response inhibition network in people with PD compared to neurotypical adults and that integrity of the response inhibition network relates to response inhibition in elderly people without PD. However, freezing status in people with PD did not impact the efficiency of response inhibition (measured via the SST), nor white matter changes in the response inhibition brain network (r-IFC, preSMA, and STN). Although preliminary, our findings do not support a cognitive inhibition deficit in people with PD and FoG.

ACKNOWLEDGMENTS

The project was supported by grants from the Medical Research Foundation of Oregon (Early Clinical Investigator award; PI: KS), the US Department of Veteran’s Affairs Rehabilitation Research and Development Service (Career Development Award-1: #I01BX007080; PI: DSP) and VA Merit Award (I01 RX001075-01; PI: FBH), the National Institutes of Health (R01 AG006457 29 PI: FH), an NIH Career Development Award K99 HD078492 0IAI (PI: MM), and NIH/NCATS (KL2TR000152; PI: BWF). The authors thank all participants for their effort, and Natassja Pal, Graham Harker, and Michael Fleming for assisting in participant recruitment, screening, and data collection.

CONFLICTS OF INTEREST

OHSU and Dr Horak have a significant financial interest in APDM, a company that may have a commercial interest in the results of this research and technology. This potential institutional and individual conflict has been reviewed and managed by OHSU.

SUPPLEMENTARY MATERIAL

To view supplementary material for this article, please visit <https://doi.org/10.1017/S135561772000123X>.

REFERENCES

- Aron, A. R., Behrens, T. E., Smith, S., Frank, M. J., & Poldrack, R. A. (2007). Triangulating a cognitive control network using diffusion-weighted magnetic resonance imaging (MRI) and functional MRI. *Journal of Neuroscience*, 27(14), 3743–3752. doi: 10.1523/JNEUROSCI.0519-07.2007
- Aron, A. R., Robbins, T. W., & Poldrack, R. A. (2014). Inhibition and the right inferior frontal cortex: One decade on. *Trends in Cognitive Sciences*, 18(4), 177–185. doi: 10.1016/j.tics.2013.12.003
- Beaulne-Seguin, Z., & Nantel, J. (2016). Conflicting and non-conflicting visual cues lead to error in gait initiation and gait inhibition in individuals with freezing of gait. *Gait & Posture*, 49, 443–447. doi: 10.1016/j.gaitpost.2016.08.002
- Behrens, T. E., Berg, H. J., Jbabdi, S., Rushworth, M. F., & Woolrich, M. W. (2007). Probabilistic diffusion tractography with multiple fibre orientations: What can we gain? *Neuroimage*, 34(1), 144–155. doi: 10.1016/j.neuroimage.2006.09.018
- Behrens, T. E., Woolrich, M. W., Jenkinson, M., Johansen-Berg, H., Nunes, R. G., Clare, S., . . . Smith, S. M. (2003). Characterization and propagation of uncertainty in diffusion-weighted MR imaging. *Magnetic Resonance in Medicine*, 50(5), 1077–1088. doi: 10.1002/mrm.10609
- Bharti, K., Suppa, A., Pietracupa, S., Upadhyay, N., Gianni, C., Leodori, G., . . . Pantano, P. (2019). Aberrant functional connectivity in patients with Parkinson’s disease and freezing of gait: A within- and between-network analysis. *Brain Imaging and Behavior*. doi: 10.1007/s11682-019-00085-9
- Bissett, P. G., Logan, G. D., van Wouwe, N. C., Tolleson, C. M., Phibbs, F. T., Claassen, D. O., & Wylie, S. A. (2015). Generalized motor inhibitory deficit in Parkinson’s disease patients who freeze. *Journal of Neural Transmission*, 122(12), 1693–1701. doi: 10.1007/s00702-015-1454-9
- Bohnen, N. I., & Albin, R. L. (2011). White matter lesions in Parkinson disease. *Nature Reviews Neurology*, 7(4), 229–236. doi: 10.1038/nrneurol.2011.21
- Boucher, L., Palmeri, T. J., Logan, G. D., & Schall, J. D. (2007). Inhibitory control in mind and brain: An interactive race model of countermanding saccades. *Psychological Review*, 114(2), 376–397. doi: 10.1037/0033-295X.114.2.376
- Claassen, D. O., van den Wildenberg, W. P., Harrison, M. B., van Wouwe, N. C., Kanoff, K., Neimat, J. S., & Wylie, S. A. (2015). Proficient motor impulse control in Parkinson disease patients with impulsive and compulsive behaviors. *Pharmacology*

- Biochemistry and Behavior*, 129, 19–25. doi: [10.1016/j.pbb.2014.11.017](https://doi.org/10.1016/j.pbb.2014.11.017)
- Coxon, J. P., Van Impe, A., Wenderoth, N., & Swinnen, S. P. (2012). Aging and inhibitory control of action: Cortico-subthalamic connection strength predicts stopping performance. *Journal of Neuroscience*, 32(24), 8401–8412. doi: [10.1523/JNEUROSCI.6360-11.2012](https://doi.org/10.1523/JNEUROSCI.6360-11.2012)
- Daividsdottir, S., Cronin-Golomb, A., & Lee, A. (2005). Visual and spatial symptoms in Parkinson's disease. *Vision Research*, 45(10), 1285–1296. doi: [10.1016/j.visres.2004.11.006](https://doi.org/10.1016/j.visres.2004.11.006)
- Di Caprio, V., Modugno, N., Mancini, C., Olivola, E., & Mirabella, G. (2020). Early-stage Parkinson's patients show selective impairment in reactive but not proactive inhibition. *Movement Disorders*, 35(3), 409–418. doi: [10.1002/mds.27920](https://doi.org/10.1002/mds.27920)
- Eagle, D. M., Bari, A., & Robbins, T. W. (2008). The neuropsychopharmacology of action inhibition: Cross-species translation of the stop-signal and go/no-go tasks. *Psychopharmacology*, 199(3), 439–456. doi: [10.1007/s00213-008-1127-6](https://doi.org/10.1007/s00213-008-1127-6)
- Eickhoff, S. B., Jbabdi, S., Caspers, S., Laird, A. R., Fox, P. T., Zilles, K., & Behrens, T. E. (2010). Anatomical and functional connectivity of cytoarchitectonic areas within the human parietal operculum. *Journal of Neuroscience*, 30(18), 6409–6421. doi: [10.1523/JNEUROSCI.5664-09.2010](https://doi.org/10.1523/JNEUROSCI.5664-09.2010)
- Factor, S. A., Scullin, M. K., Sollinger, A. B., Land, J. O., Wood-Siverio, C., Zanders, L., ... Goldstein, F. C. (2014). Freezing of gait subtypes have different cognitive correlates in Parkinson's disease. *Parkinsonism & Related Disorders*, 20(12), 1359–1364. doi: [10.1016/j.parkreldis.2014.09.023](https://doi.org/10.1016/j.parkreldis.2014.09.023)
- Fearon, C., Butler, J. S., Newman, L., Lynch, T., & Reilly, R. B. (2015). Audiovisual processing is abnormal in Parkinson's disease and correlates with freezing of gait and disease duration. *Journal of Parkinson's Disease*, 5(4), 925–936. doi: [10.3233/JPD-150655](https://doi.org/10.3233/JPD-150655)
- Fling, B. W., Cohen, R. G., Mancini, M., Carpenter, S. D., Fair, D. A., Nutt, J. G., & Horak, F. B. (2014). Functional reorganization of the locomotor network in Parkinson patients with freezing of gait. *PLoS One*, 9(6), e100291. doi: [10.1371/journal.pone.0100291](https://doi.org/10.1371/journal.pone.0100291)
- Fling, B. W., Cohen, R. G., Mancini, M., Nutt, J. G., Fair, D. A., & Horak, F. B. (2013). Asymmetric pedunculopontine network connectivity in parkinsonian patients with freezing of gait. *Brain*, 136(Pt 8), 2405–2418. doi: [10.1093/brain/awt172](https://doi.org/10.1093/brain/awt172)
- Gauggel, S., Rieger, M., & Feghoff, T. A. (2004). Inhibition of ongoing responses in patients with Parkinson's disease. *Journal of Neurology, Neurosurgery and Psychiatry*, 75(4), 539–544. doi: [10.1136/jnnp.2003.016469](https://doi.org/10.1136/jnnp.2003.016469)
- Georgiades, M. J., Gilat, M., Ehgoetz Martens, K. A., Walton, C. C., Bissett, P. G., Shine, J. M., & Lewis, S. J. (2016). Investigating motor initiation and inhibition deficits in patients with Parkinson's disease and freezing of gait using a virtual reality paradigm. *Neuroscience*, 337, 153–162. doi: [10.1016/j.neuroscience.2016.09.019](https://doi.org/10.1016/j.neuroscience.2016.09.019)
- Gilat, M., Shine, J. M., Walton, C. C., O'Callaghan, C., Hall, J. M., & Lewis, S. J. G. (2015). Brain activation underlying turning in Parkinson's disease patients with and without freezing of gait: A virtual reality fMRI study. *npj Parkinson's Disease*, 1, 15020. doi: [10.1038/npjparkd.2015.20](https://doi.org/10.1038/npjparkd.2015.20)
- Goetz, C. G., Tilley, B. C., Shaftman, S. R., Stebbins, G. T., Fahn, S., Martinez-Martin, P., ... Movement Disorder Society, U. R. T. F. (2008). Movement Disorder Society-sponsored revision of the Unified Parkinson's Disease Rating Scale (MDS-UPDRS): Scale presentation and clinimetric testing results. *Movement Disorders*, 23(15), 2129–2170. doi: [10.1002/mds.22340](https://doi.org/10.1002/mds.22340)
- Hair, J., Anderson, R., Tatham, R., & Black, W. (1998). Multivariate data analysis (5 ed.). Englewood Cliffs, NJ: Prentice-Hall.
- Hoehn, F., Barnea-Goraly, N., Haas, B. W., Golarai, G., Ng, D., Mills, D., ... Reiss, A. L. (2007). More is not always better: Increased fractional anisotropy of superior longitudinal fasciculus associated with poor visuospatial abilities in Williams syndrome. *Journal of Neuroscience*, 27(44), 11960–11965. doi: [10.1523/JNEUROSCI.3591-07.2007](https://doi.org/10.1523/JNEUROSCI.3591-07.2007)
- Hoehn, M. M., & Yahr, M. D. (1967). Parkinsonism: Onset, progression and mortality. *Neurology*, 17(5), 427–442. doi: [10.1212/wnl.17.5.427](https://doi.org/10.1212/wnl.17.5.427)
- Hughes, A. J., Daniel, S. E., Kilford, L., & Lees, A. J. (1992). Accuracy of clinical diagnosis of idiopathic Parkinson's disease: A clinico-pathological study of 100 cases. *Journal of Neurology, Neurosurgery and Psychiatry*, 55(3), 181–184.
- Isaacs, B. R., Trutti, A. C., Pelzer, E., Tittgemeyer, M., Temel, Y., Forstmann, B. U., & Keuken, M. C. (2019). Cortico-basal white matter alterations occurring in Parkinson's disease. *PLoS One*, 14(8), e0214343. doi: [10.1371/journal.pone.0214343](https://doi.org/10.1371/journal.pone.0214343)
- Kohl, S., Aggeli, K., Obeso, I., Speekenbrink, M., Limousin, P., Kuhn, J., & Jahanshahi, M. (2015). In Parkinson's disease pallidal deep brain stimulation speeds up response initiation but has no effect on reactive inhibition. *Journal of Neurology*, 262(7), 1741–1750. doi: [10.1007/s00415-015-7768-6](https://doi.org/10.1007/s00415-015-7768-6)
- Lewis, S. J., & Barker, R. A. (2009). A pathophysiological model of freezing of gait in Parkinson's disease. *Parkinsonism & Related Disorders*, 15(5), 333–338. doi: [10.1016/j.parkreldis.2008.08.006](https://doi.org/10.1016/j.parkreldis.2008.08.006)
- Mancini, M., Smulders, K., Cohen, R. G., Horak, F. B., Giladi, N., & Nutt, J. G. (2017). The clinical significance of freezing while turning in Parkinson's disease. *Neuroscience*, 343, 222–228. doi: [10.1016/j.neuroscience.2016.11.045](https://doi.org/10.1016/j.neuroscience.2016.11.045)
- Manza, P., Schwartz, G., Masson, M., Kann, S., Volkow, N. D., Li, C. R., & Leung, H. C. (2018). Levodopa improves response inhibition and enhances striatal activation in early-stage Parkinson's disease. *Neurobiology of Aging*, 66, 12–22. doi: [10.1016/j.neurobiolaging.2018.02.003](https://doi.org/10.1016/j.neurobiolaging.2018.02.003)
- Morris, R., Smulders, K., Peterson, D. S., Mancini, M., Carlson-Kuhta, P., Nutt, J. G., & Horak, F. B. (2020). Cognitive function in people with and without freezing of gait in Parkinson's disease. *npj Parkinson's Disease*, 6, 9. doi: [10.1038/s41531-020-0111-7](https://doi.org/10.1038/s41531-020-0111-7)
- Naismith, S. L., Shine, J. M., & Lewis, S. J. (2010). The specific contributions of set-shifting to freezing of gait in Parkinson's disease. *Movement Disorders*, 25(8), 1000–1004. doi: [10.1002/mds.23005](https://doi.org/10.1002/mds.23005)
- Nasreddine, Z. S., Phillips, N. A., Bedirian, V., Charbonneau, S., Whitehead, V., Collin, I., ... Chertkow, H. (2005). The Montreal Cognitive Assessment, MoCA: A brief screening tool for mild cognitive impairment. *Journal of the American Geriatrics Society*, 53(4), 695–699. doi: [10.1111/j.1532-5415.2005.53221.x](https://doi.org/10.1111/j.1532-5415.2005.53221.x)
- Nieuwboer, A., & Giladi, N. (2013). Characterizing freezing of gait in Parkinson's disease: Models of an episodic phenomenon. *Movement Disorders*, 28(11), 1509–1519. doi: [10.1002/mds.25683](https://doi.org/10.1002/mds.25683)
- Nieuwboer, A., Rochester, L., Herman, T., Vandenbergh, W., Emil, G. E., Thomaes, T., & Giladi, N. (2009). Reliability of the new freezing of gait questionnaire: Agreement between patients with Parkinson's disease and their carers. *Gait & Posture*, 30(4), 459–463. doi: [10.1016/j.gaitpost.2009.07.108](https://doi.org/10.1016/j.gaitpost.2009.07.108)
- Nutt, J. G., Bloem, B. R., Giladi, N., Hallett, M., Horak, F. B., & Nieuwboer, A. (2011). Freezing of gait: Moving forward on a

- mysterious clinical phenomenon. *The Lancet Neurology*, 10(8), 734–744. doi: [10.1016/S1474-4422\(11\)70143-0](https://doi.org/10.1016/S1474-4422(11)70143-0)
- Obeso, I., Wilkinson, L., Casabona, E., Bringas, M. L., Alvarez, M., Alvarez, L., . . . Jahanshahi, M. (2011). Deficits in inhibitory control and conflict resolution on cognitive and motor tasks in Parkinson's disease. *Experimental Brain Research*, 212(3), 371–384. doi: [10.1007/s00221-011-2736-6](https://doi.org/10.1007/s00221-011-2736-6)
- Obeso, I., Wilkinson, L., Casabona, E., Speekenbrink, M., Luisa Bringas, M., Alvarez, M., . . . Jahanshahi, M. (2014). The subthalamic nucleus and inhibitory control: Impact of subthalamotomy in Parkinson's disease. *Brain*, 137(Pt 5), 1470–1480. doi: [10.1093/brain/awu058](https://doi.org/10.1093/brain/awu058)
- Rae, C. L., Hughes, L. E., Anderson, M. C., & Rowe, J. B. (2015). The prefrontal cortex achieves inhibitory control by facilitating subcortical motor pathway connectivity. *Journal of Neuroscience*, 35(2), 786–794. doi: [10.1523/JNEUROSCI.3093-13.2015](https://doi.org/10.1523/JNEUROSCI.3093-13.2015)
- Shine, J. M., Naismith, S. L., Palavra, N. C., Lewis, S. J., Moore, S. T., Dilda, V., & Morris, T. R. (2013). Attentional set-shifting deficits correlate with the severity of freezing of gait in Parkinson's disease. *Parkinsonism & Related Disorders*, 19(3), 388–390. doi: [10.1016/j.parkreldis.2012.07.015](https://doi.org/10.1016/j.parkreldis.2012.07.015)
- Smulders, K., Esselink, R. A., Bloem, B. R., & Cools, R. (2015). Freezing of gait in Parkinson's disease is related to impaired motor switching during stepping. *Movement Disorders*, 30(8), 1090–1097. doi: [10.1002/mds.26133](https://doi.org/10.1002/mds.26133)
- Snijders, A. H., Takakusaki, K., Debu, B., Lozano, A. M., Krishna, V., Fasano, A., . . . Hallett, M. (2016). Physiology of freezing of gait. *Annals of Neurology*, 80(5), 644–659. doi: [10.1002/ana.24778](https://doi.org/10.1002/ana.24778)
- Stefanova, E., Lukic, M. L. Z., Markovic, V., Stojkovic, T., Tomic, A., . . . Kostic, V. (2014). Acquisition and discrimination set learning deficits in Parkinson's disease with freezing of gait. *Journal of the International Neuropsychological Society*, 20(9), 929–936.
- Sylvester, C. Y., Wager, T. D., Lacey, S. C., Hernandez, L., Nichols, T. E., Smith, E. E., & Jonides, J. (2003). Switching attention and resolving interference: fMRI measures of executive functions. *Neuropsychologia*, 41(3), 357–370. doi: [10.1016/s0028-3932\(02\)00167-7](https://doi.org/10.1016/s0028-3932(02)00167-7)
- Uribe, C., Segura, B., Baggio, H. C., Abos, A., Garcia-Diaz, A. I., Campabadal, A., . . . Junque, C. (2018). Gray/white matter contrast in Parkinson's disease. *Frontiers in Aging Neuroscience*, 10, 89. doi: [10.3389/fnagi.2018.00089](https://doi.org/10.3389/fnagi.2018.00089)
- Vandenbossche, J., Deroost, N., Soetens, E., Spildooren, J., Vercruysse, S., Nieuwboer, A., & Kerckhofs, E. (2011). Freezing of gait in Parkinson disease is associated with impaired conflict resolution. *Neurorehabilitation and Neural Repair*, 25(8), 765–773. doi: [10.1177/1545968311403493](https://doi.org/10.1177/1545968311403493)
- Verbruggen, F., Aron, A. R., Band, G. P., Beste, C., Bissett, P. G., Brockett, A. T., . . . Boehler, C. N. (2019). A consensus guide to capturing the ability to inhibit actions and impulsive behaviors in the stop-signal task. *Elife*, 8. doi: [10.7554/eLife.46323](https://doi.org/10.7554/eLife.46323)
- Verbruggen, F., Chambers, C. D., & Logan, G. D. (2013). Fictitious inhibitory differences: How skewness and slowing distort the estimation of stopping latencies. *Psychological Science*, 24(3), 352–362. doi: [10.1177/0956797612457390](https://doi.org/10.1177/0956797612457390)
- Verbruggen, F., Logan, G. D., & Stevens, M. A. (2008). STOP-IT: Windows executable software for the stop-signal paradigm. *Behavior Research Methods*, 40(2), 479–483.
- Vercruysse, S., Leunissen, I., Vervoort, G., Vandenberghe, W., Swinnen, S., & Nieuwboer, A. (2015). Microstructural changes in white matter associated with freezing of gait in Parkinson's disease. *Movement Disorders*, 30(4), 567–576. doi: [10.1002/mds.26130](https://doi.org/10.1002/mds.26130)
- Vriend, C., Gerrits, N. J., Berendse, H. W., Veltman, D. J., van den Heuvel, O. A., & van der Werf, Y. D. (2015). Failure of stop and go in de novo Parkinson's disease – a functional magnetic resonance imaging study. *Neurobiology of Aging*, 36(1), 470–475. doi: [10.1016/j.neurobiolaging.2014.07.031](https://doi.org/10.1016/j.neurobiolaging.2014.07.031)
- Walton, C. C., Shine, J. M., Hall, J. M., O'Callaghan, C., Mowszowski, L., Gilat, M., . . . Lewis, S. J. (2015). The major impact of freezing of gait on quality of life in Parkinson's disease. *Journal of Neurology*, 262(1), 108–115. doi: [10.1007/s00415-014-7524-3](https://doi.org/10.1007/s00415-014-7524-3)
- Wessel, J. R., & Aron, A. R. (2015). It's not too late: The onset of the frontocentral P3 indexes successful response inhibition in the stop-signal paradigm. *Psychophysiology*, 52(4), 472–480. doi: [10.1111/psyp.12374](https://doi.org/10.1111/psyp.12374)
- Wylie, S. A., van Wouwe, N. C., Godfrey, S. G., Bissett, P. G., Logan, G. D., Kanoff, K. E., . . . van den Wildenberg, W. P. M. (2018). Dopaminergic medication shifts the balance between going and stopping in Parkinson's disease. *Neuropsychologia*, 109, 262–269. doi: [10.1016/j.neuropsychologia.2017.12.032](https://doi.org/10.1016/j.neuropsychologia.2017.12.032)